Title

Microphase Behavior and Enhanced Wet-Cohesion of Synthetic Copolyampholytes Inspired by a Mussel Foot Protein

Journal

Journal of the American Chemical Society, 137(29)

ISSN

0002-7863

Authors

Seo, Sungbaek
Das, Saurabh
Zalicki, Piotr J
et al.

Publication Date

2015-07-29

DOI

10.1021/jacs.5b03827

Peer reviewed

JACS
JOURNAL OF THE AMERICAN CHEMICAL SOCIETY

Communication

pubs.acs.org/JACS

Microphase Behavior and Enhanced Wet-Cohesion of Synthetic Copolyampholytes Inspired by a Mussel Foot Protein

Sungbaek Seo,[†,#] Saurabh Das,[†,‡,#] Piotr J. Zalicki,[†,§] Razieh Mirshafian,[†] Claus D. Eisenbach,[∥,⊥] Jacob N. Israelachvili,[‡] J. Herbert Waite,[†,§] and B. Kollbe Ahn*[,†]

[†]Marine Science Institute, [‡]Chemical Engineering, [§]Molecular, Cellular and Developmental Biology, and [∥]Materials Research Laboratory, University of California, Santa Barbara, California 93106, United States

[⊥]Institute for Polymer Chemistry, University of Stuttgart, D-70569 Stuttgart, Germany

Supporting Information

ABSTRACT: Numerous attempts have been made to translate mussel adhesion to diverse synthetic platforms. However, the translation remains largely limited to the Dopa (3,4-dihydroxyphenylalanine) or catechol functionality, which continues to raise concerns about Dopa's inherent susceptibility to oxidation. Mussels have evolved adaptations to stabilize Dopa against oxidation. For example, in mussel foot protein 3 *slow* (mfp-3s, one of two electrophoretically distinct interfacial adhesive proteins in mussel plaques), the high proportion of hydrophobic amino acid residues in the flanking sequence around Dopa increases Dopa's oxidation potential. In this study, copolyampholytes, which combine the catechol functionality with amphiphilic and ionic features of mfp-3s, were synthesized and formulated as coacervates for adhesive deposition on surfaces. The ratio of hydrophilic/hydrophobic as well as cationic/anionic units was varied in order to enhance coacervate formation and wet adhesion properties. Aqueous solutions of two of the four mfp-3s-inspired copolymers showed coacervate-like spherical microdroplets ($\phi \approx 1-5$ μm at pH ~4 (salt concentration ~15 mM). The mfp-3s-mimetic copolymer was stable to oxidation, formed coacervates that spread evenly over mica, and strongly bonded to mica surfaces (pull-off strength: ~17.0 mJ/m^2). Increasing pH to 7 after coacervate deposition at pH 4 doubled the bonding strength to ~32.9 mJ/m^2 without oxidative cross-linking and is about 9 times higher than native mfp-3s cohesion. This study expands the scope of translating mussel adhesion from simple Dopa-functionalization to mimicking the context of the local environment around Dopa.

Marine mussels (Figure 1a) attach to hard surfaces, e.g., mineral and metal, in the intertidal zone where waves with and without suspended sand often exceed 25 m/sec velocities. 3,4-Dihydroxyphenylalanine (Dopa), a main constituent in mussel foot proteins (mfps) and substantially contributing to wet adhesion, has been incorporated in synthetic polymers to mimic the bio wet-adhesion.[1−5] However, other constitutional features of mfps, e.g., cationic residues (lysine, K), anionic residues (aspartic acid, D), nonionic polar residues (asparagine, N), and nonpolar residues (alanine, A), have not typically been included in mussel-inspired synthetic wet-adhesion systems.[1,2]

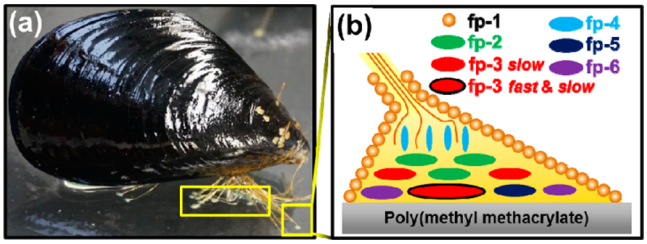

Figure 1. Marine mussel and the approximate location of mussel foot proteins in the byssus. (a) *Mytilus californianus* attached to poly(methyl methacrylate) surface. (b) Schematic of the types and distribution of mfps.

Here, we studied the microphase behavior and wet-adhesion of copolyampholytes with fixed catechol content and varied other key functionalities. Potential effects of aromatic moieties (Tyr, Trp) besides Dopa in mfp-3s have not been specifically tested in the present structural design of the model copolyampholytes. Conditions for the experiments were adjusted according to the microenvironmental conditions of adhesive protein deposition under the mussel's foot including acidic to neutral pH and ionic strength of ≤100 mM.[3,4]

In mussel adhesion, polyelectrolyte adhesive proteins or mfps are presented to target surfaces after being condensed as a dense fluid by complex coacervation, a critical step in the formation of protein-based underwater adhesives.[5] The first synthetic adhesive to be studied as a complex coacervate was modeled after sandcastle worm cement and consisted of two oppositely charged dopamine-functionalized polyelectrolytes.[6,7] Coacervation benefits adhesion in several important ways: (1) high polymer concentration increases density, (2) the low interfacial energy improves wetting, (3) high diffusivity maintains good mixing, and (4) reduced viscosity eases delivery.[1]

Mfp-3s is localized to the plaque−substratum interface (Figure 1b) together with mfp-3f and mfp-5. Due to its amphiphilic and ampholytic structural characteristics (Figure 2a), mfp-3s is capable of self-coacervation[8] and is more stable at oxidation than other mfps.[9] Intrigued by mfp-3s's (molecular weight ~5 kDa) unique property to self-coacervate, we synthesized a series of ampholytic copolymers consisting of randomly arranged catechol (M1)-functionalized, cationic (M2), anionic (M3),

Received: April 20, 2015
Published: July 14, 2015

DOI: 10.1021/jacs.5b03827
J. Am. Chem. Soc. 2015, 137, 9214−9217

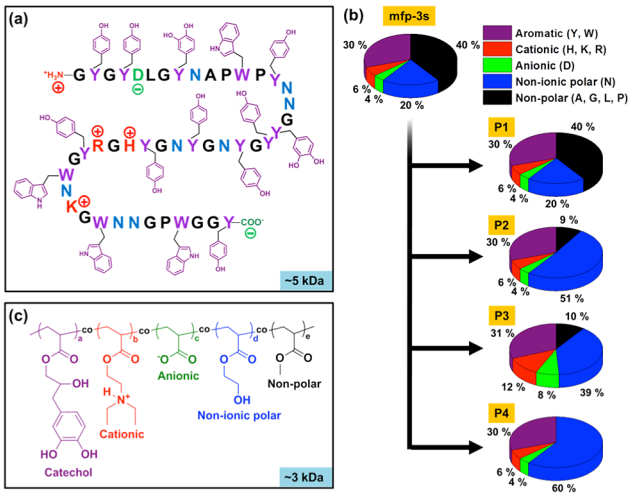

Figure 2. Key features of mfps and synthetic homologs. (a) Primary sequence of mfp-3s. (b) Pie chart of key functionalities in mfp-3s and synthetic analogues: copolymer 1 (P1) to copolymer 4 (P4). (c) Chemical composition of a copolyacrylate with randomly distributed mfp-3s-mimetic functionalities.

nonionic hydrophilic (M4), and hydrophobic (M5) comonomer units (Figure 2b,c). These synthetic copolyampholytes of fixed catechol content and varied ratio of hydrophilic/hydrophobic as well as acid/base units (Figure 2b) carry key constituent features of mfp-3s. Copolymer 1 (P1) was synthesized following the ratio of catecholic, cationic, anionic, nonionic polar, and nonpolar amino acid units of mfp-3s. In copolymer 2 (P2), hydrophobicity was decreased by increasing the fraction of nonionic polar (P; hydrophilic) groups (comonomer M4) at the expense of nonpolar (NP; hydrophobic) groups (comonomer M5). In copolymer 3 (P3), the overall charge density was increased by doubling the levels of both cationic and anionic residues by keeping the total fraction of comonomers M2, M3, and M4 the same as in P2. In copolymer 4 (P4), in comparison to P1 the nonpolar hydrophobic residue (comonomer M5) was completely omitted, i.e., its intrinsic hydrophobicity originates from the polymer backbone, which is hydrophilic (peptide linkage) in mfps.

The literature on synthetic ampholytic copolymers in aqueous solution contains only one example where liquid−liquid phase separation was observed: Copolymers with 60/40 (or 35/65) mole ratios in their acid/base repeat unit exhibited a two-phase liquid−liquid system at low salinity, whereas all other copolymer compositions gave either solid−liquid two-phase systems or were completely soluble, irrespective of the ion strength.[10] In other words, the coacervation-reminiscent phase behavior occurred only in a relatively narrow nonstoichiometric acid/base comonomer ratio range. In the light of these findings and also considering the unequal content of anionic and cationic residues in mfp-3s (4 vs 6 mol %),[11] the acid/base comonomer ratios of the copolyampholytes synthesized in this study were adjusted accordingly: 6 and 4 mol % cationic and anionic units, respectively, as in mfp-3s, or twice as high at 12 and 8 mol %, respectively.

Building upon the thoroughly investigated complex coacervation between poly(acrylic acid) and poly(2-dimethyl aminoethyl methacrylate) or poly(allyl amine),[11,12] acrylic acid (AA), and 2-(diethylamino)ethyl acrylate (DEAEA) were chosen as oppositely charged comonomers in the synthesis of the copolyampholytes (Figure 2c). The specific functional groups in the model copolymers differ from those in mfp-3s due to the different nature of the polymer backbones and side chain chemistry; however, overall structural tendencies are preserved. The primary objective here is not to mimic specific functionalities in mfp-3s but to produce a relatively simple and inexpensive model polymer for fundamental structure−properties studies. Inspired by the nonrepetitive amino acid sequence of mfp-3s (Figure 2a),[9] random copolymers were synthesized via free radical copolymerization. Random monomer distribution of the copolymers was confirmed by monitoring the copolymerization from time zero through 15, 30, 45, 60, and 720 min: samples taken from the reaction mixture were analyzed by gas chromatography (GC), gel permeation chromatography (GPC), and nuclear magnetic resonance spectroscopy (NMR). Details of the analytical protocols regarding monomer conversion (or consumption) determined by GC, polymer yield and total nonvolatile monomer conversion determined by GPC, and copolymer composition determined by NMR are given in the Supporting Information (SI). The composition of the copolymer was consistent during the entire reaction, demonstrating the random comonomer distribution along the copolymer chains. The copolyampholytes were obtained after removal of the protective groups from these precursor copolymers (see SI for details).

The microphase behavior of aqueous solutions of the deprotected copolyampholyte, i.e., occurrence of a single-phase solution, liquid−liquid (coacervation), or liquid−solid (precipitation) two-phase separation was investigated and related to the wet adhesive properties of the materials. Increasing the mole ratio P/NP of nonionic polar (hydrophilic; M4 based) and nonpolar (hydrophobic; M5 based) comonomers from 20/40 to 60/0 in the copolymer increased its water solubility gradually from 0 to 0.5 wt % at pH > 8, where the tertiary-amino group of DEAEA-based repeat units start to be deprotonated. Hence the polymer concentration used in this study was 0.01 wt %. Whereas both P2 and P4 showed dynamic microphase behavior, both P1 and P3 were insoluble. P2 and P4, however, were soluble only at pH ≥ 8 due to charge screening, hence a slight concentration of Na^+ and Cl^- inevitably was accumulated after adjusting the pH of the solution by addition of 0.1 M NaOH or HCl (see SI for more details). The insolubility of P1 in aqueous medium is attributed to its high content of hydrophobic M5 comonomer. This is supported by the solubility of P2, which differs from P1 by the distinct increase in the content of the hydrophilic M4-based comonomer and corresponding decrease of M5 comonomer. In comparison to P2, increasing charge densities (doubling of both positive and negative charges) to the expense of nonionic hydrophilic M4-based comonomer in P3 resulted in precipitation. This is attributed to an increased number of short-range electrostatic interactions between acid and base side groups.[13]

At pH ≈ 4 (salt concentration ≈ 15 mM), both P2 and P4 showed spherical microdroplets (coacervates: $\phi \approx 1-5$ μm) (Figure 3a). However, at pH ≈ 3 (salt concentration ~20 mM), the copolymers precipitated (Figure 3a). This is a consequence of protonation of carboxylate side-chains, as pH was decreased below the pK_a (~4) of carboxylic groups in the copolymer chain. At pH ≥ 7 (salt concentration ≤ 5 mM), particularly at pH close to the pK_a (~8) of DEAEA, a single phase solution of the copolymer was obtained as inferred from both the micrograph (Figure 3a) and turbidity data (Figure 3b). The phase behavior at pH 2 to 9 (salt concentration ≤ 20 mM) (Figure 3a,b) described above was identical to that measured at a fixed ionic strength of ~10 mM. Similarly, mfp-3s showed dynamic microphase behavior at pH 3 to 7.5 at ionic strengths ≤ 100 mM.[8] We also studied phase

DOI: 10.1021/jacs.5b03827
J. Am. Chem. Soc. 2015, 137, 9214−9217

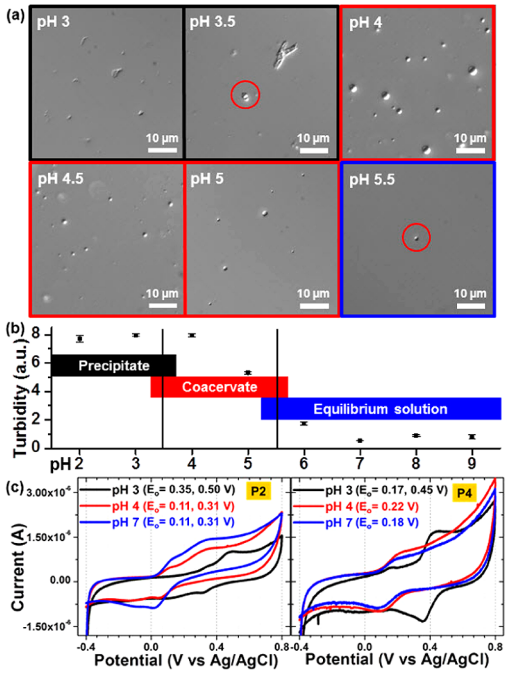

Figure 3. Microphase behavior and cyclic voltammograms (CV) of mfp-3s-mimetic copolyampholytes. (a) Light microscopic images of P2 at pH 3, 3.5, 4, 4.5, 5, and 5.5 (images for P4 not shown, followed same trend). (b) Turbidity of 0.01 wt % P2 in H_2O at pH 2−9 (data for P4 not shown, followed same trend). (c) CV of 0.01 wt % P2 (upper panel) and P4 (lower panel), respectively, in H_2O at pH 3, 4, and 7.

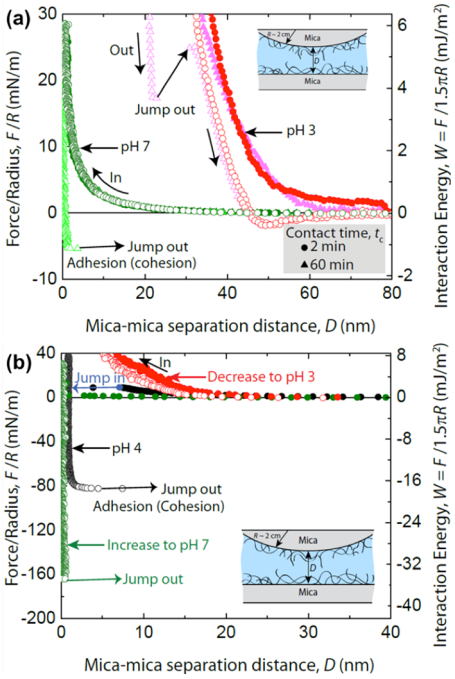

Figure 4. Representative force vs distance plots between P2 films absorbed onto mica in SFA. (a) Interaction energy (cohesion) between P2 films on mica, adsorbed and measured at pH 3 and 7, respectively. (b) Interaction energy between P2 films on mica, measured at pH 4 (black), pH 3 (red), and pH 7 (green), respectively, after adsorption at pH 4.

behavior of the coacervate formed at pH 4 as a function of salt concentration. The copolymer started to precipitate above 100 mM salt where precipitation is attributed to decreasing the solvent quality (aq. NaCl solution) for the copolyampholyte with increasing salt concentration.[11]

Cyclic voltammetry (CV) of P2 (more hydrophobic) showed an oxidation potential (E_0) of catechol, ~0.50 V at pH 3 and ~0.31 V at pH 4 and 7 (Figure 3c), similar to E_0 of Dopa in mfp-3s, ~0.5 V at pH 2 and ~0.35 V at pH 7.5.[9] These are significantly higher than E_0 of catechol in P4 (less hydrophobic), ~0.45 V at pH 3, ~0.22 V at pH 4, and ~0.18 V at pH 7 (Figure 3c). In the CV of P2, the amount of catecholic and vinyl-catecholic (an α,β-dehydro derivative of Dopa oxidation in mfps that arises from quinone tautomerization)[14] functionalities at pH 4 was similar to that at pH 7, whereas P4 did not exhibit the vinyl-catechol at pH 4 and 7. Comparable experiments carried out between P2 and P4 showed an oxidation inhibiting effect of hydrophobic comonomer units. UV−vis absorption spectra (see Figure S13) at pH 3, 4, and 7 also show similar amounts of catechol (~280 nm) and vinyl-catechol (320−330 nm), whereas no quinone (~390 nm) was observed even at pH 7, where Dopa oxidation occurs generally. The CV and UV−vis results suggest the high proportion of hydrophobic residues in the copolymer provides stability against catechol oxidation by shielding from the solvent just as mfp-3s showed its ability to maintain adhesion at neutral pH with comparable oxidative stability.[9]

The surface forces apparatus (SFA) was used to investigate the cohesion of the copolyampholytes (P2 and P4, respectively) adsorbed onto molecularly smooth mineral surfaces (e.g., mica) at pH 3, 4, and 7, respectively, (please see SI for more details about SFA). Hard-wall thickness of the copolyampholytes was also measured as the limiting distance between the mica surfaces during the approach run in the SFA. Representative force−distance curves between two mica surfaces coated with P2 at different pH are shown in Figure 4. In the SFA, adhesion refers to the attraction between two different surfaces, whereas cohesion is between two similar surfaces. Although P2 and P4 showed identical microphase behaviors, only P2 exhibited cohesion in the SFA at pH 4 (optimized coacervation condition for both P2 and P4). Hence our further studies focused on P2. The cohesive strength between the adsorbed films (of P2) as measured in the SFA in this study was independent of the contact time (t_c) and equilibration time (t_e) except at pH 7, where the cohesion increased with t_e. As shown in Figure 4, the polymer films, adsorbed and measured at pH 3, exhibited a relatively thick hard-wall (~20 nm) with evident repulsion beginning at surface separations of 80 nm and very low cohesion (W_c < 0.1 mJ/m^2, t_c and t_e independent). This is understood when considering that the copolymer precipitated at pH 3, and the measured data reflect the hard contact with nonsticky deposits of bulk copolymer on the mica surfaces (see AFM data in the SI). However, the polymer films adsorbed and measured at pH 4 or 7, i.e., from the two-phase liquid−liquid system, resulted in very thin hard-walls (<1 nm), reminiscent of monomolecular films between the mica surfaces. However, there was a difference between pH 4 and 7 during approach. Although polymer layers adsorbed at both pH 4 and 7 exhibited repulsion starting at ~20 nm distance indicating the thickness of the Langmuir adsorption layer, the films adsorbed at pH 7 show a stronger repulsion starting at $D \approx 20$ nm on approach, whereas the films adsorbed at pH 4 exhibited jump-in instability (due to strong attractive interaction between the surface films during approach of the surfaces) at $D \approx 7$ nm distance from the final hard-wall (black solid circles in Figure 4b). The cohesion of the films adsorbed and measured at pH 4 (17.0 ± 2.5 mJ/m^2, t_c independent) surpassed the maxima of mfp-5 (13.7 ± 0.5 mJ/m^2, $t_c \geq 1$ h), the most adhesive protein tested.[15]

DOI: 10.1021/jacs.5b03827
J. Am. Chem. Soc. 2015, 137, 9214−9217

However, the cohesion (t_c independent) of the films adsorbed and measured at pH 7 increased monotonically with t_e from no cohesion ($t_e \approx 2-10$ min) to 1.6 ± 0.4 mJ/m^2 ($t_e \approx 60$ min), 15.2 ± 0.4 mJ/m^2 ($t_e \approx 360$ min), and 24.3 ± 1.2 mJ/m^2 ($t_e \geq 1080$ min). This t_e-dependent cohesion at pH 7 suggests that the solution pH not only affects adsorption but also the cohesion of the polymer films due to changing conformation of the residues responsible for the bridging of the surface films or the adhesion to mica surface. As shown by the SFA, AFM measurements (see Figure S12) confirmed that the copolymer coated the mica surface more effectively at pH 4 (coacervate) than at pH 7 (a single phase solution) or at pH 3 (precipitate). Coating patches (<3 nm) that persist on mica after thorough rinsing were observed only when the mica was coated with the coacervate but not with the soluble phase or precipitates (please see SI for more details).

To further investigate pH effects on the cohesion of the films adsorbed onto mica at pH 4 (coacervate), the cohesion was measured under a new pH condition (no salt pH 3 or 7) after the adsorption (Figure 4b). For the films absorbed at pH 4, the cohesion was t_c independent regardless of the changed pH condition. The cohesive interaction between the polymer films disappeared at pH 3, whereas cohesion increased to 32.9 ± 3.5 mJ/m^2 at pH 7. The cohesion between the films, adsorbed (coacervate) at pH 4 and measured at pH 7 (32.9 ± 3.5 mJ/m^2), was ~1.4 times greater than that adsorbed at pH 7 (a single soluble phase) and measured at pH 7 with $t_e \geq 18$ h (24.3 ± 1.2 mJ/m^2).

The SFA and AFM results demonstrate that coacervation is essential for uniform coating of the mica surface and for obtaining higher cohesion. When adsorbed at pH 4 and re-equilibrated to pH 7, the stronger cohesion between the polymer films at the higher pH 7 may be due to the decreased Coulombic repulsion since the isoelectric point of the polymer is near neutral pH (pI 6.7). The weak repulsive forces between the polymer films can be translated into a surface charge density of 0.03 C/m^2 (surface potential, $\psi = 120$ mV) and 0.018 C/m^2 ($\psi = 40$ mV) at pH 4 and pH 7, respectively.[16] Also, the strong cohesion at pH 7 was reversible (i.e., similar cohesion forces were measured during subsequent approach−separation force runs at the same contact point with no material transfer across surfaces), suggesting Dopa−Dopaquinone induced cross-linking between the films was not the operative mechanism of cohesion. CV and UV−vis measurements confirm the absence of Dopa−Dopaquinone induced cross-linking to the strong cohesion at neutral pH. The levels of catechol and vinyl-catechol in the polymer at pH 4 were similar to those at pH 7, and there were no oxidative products of catechol (e.g., quinone) at pH 4 nor even at pH 7, where catechol (or Dopa) oxidation typically occurs. This oxidation stability could be due to hydrophobic or electrophilic shielding of the Dopa moieties as proposed for mfp-3s.[9]

This study emphasizes the importance of the balance between electrostatic and hydrophobic interactions for coacervation and wet-adhesion in addition to catecholic interactions, e.g., oxidative cross-linking,[17,18] metal coordination,[19,20] and intermolecular hydrogen bonding.[21] The mfp-3s-mimetic copolyampholyte has potential as a high performance wet adhesive/coating with its very strong wet-cohesion (~8.8, ~2.4, and ~1.6 times greater than mfp-3s,[9] mfp-5,[15] the most adhesive natural protein, and the recently engineered mfp-amyloid protein,[22] respectively) and stable coacervation. This study expands the scope of translation of the biological organism by combining Dopa with hydrophobic and electrostatic functionalities.

■ ASSOCIATED CONTENT

Supporting Information

Additional information and experimental methods. The Supporting Information is available free of charge on the ACS Publications website at DOI: 10.1021/jacs.5b03827.

■ AUTHOR INFORMATION

Corresponding Author

*ahn@lifesci.ucsb.edu

Author Contributions

#S.S. and S.D. contributed equally to this work.

Notes

The authors declare no competing financial interest.

■ ACKNOWLEDGMENTS

The authors gratefully acknowledge financial support from Office of Naval Research N000141310867 and National Science Foundation MRSEC DMR-1121053. Authors wish to thank Mary Raven in NRI/MCDB Microscopy Facility (NIH 1 S10 OD010610-01A1), Rachel Berhrens in MRL, and Bruce Lipshutz for the use of his autocolumn.

■ REFERENCES

(1) Stewart, R. J.; Ransom, T. C.; Hlady, V. *J. Polym. Sci., Part B: Polym. Phys.* **2011**, *49*, 757.

(2) Faure, E.; Falentin-Daudré, C.; Jérôme, C.; Lyskawa, J.; Fournier, D.; Woisel, P.; Detrembleur, C. *Prog. Polym. Sci.* **2013**, *38*, 236.

(3) Martinez Rodriguez, N. R.; Das, S.; Kaufman, Y.; Israelachvili, J. N.; Waite, J. H. *Biofouling* **2015**, *31*, 221.

(4) Yu, J.; Wei, W.; Danner, E.; Ashley, R. K.; Israelachvili, J. N.; Waite, J. H. *Nat. Chem. Biol.* **2011**, *7*, 588.

(5) Ortony, J. H.; Hwang, D. S.; Franck, J. M.; Waite, J. H.; Han, S. *Biomacromolecules* **2013**, *14*, 1395.

(6) Shao, H.; Stewart, R. J. *Adv. Mater.* **2010**, *22*, 729.

(7) Shao, H.; Bachus, K. N.; Stewart, R. J. *Macromol. Biosci.* **2009**, *9*, 464.

(8) Wei, W.; Tan, Y.; Martinez Rodriguez, N. R.; Yu, J.; Israelachvili, J. N.; Waite, J. H. *Acta Biomater.* **2014**, *10*, 1663.

(9) Wei, W.; Yu, J.; Broomell, C.; Israelachvili, J. N.; Waite, J. H. *J. Am. Chem. Soc.* **2013**, *135*, 377.

(10) Corpart, J. M.; Candau, F. *Macromolecules* **1993**, *26*, 1333.

(11) Spruijt, E.; Westphal, A. H.; Borst, J. W.; Cohen Stuart, M. A.; van der Gucht, J. *Macromolecules* **2010**, *43*, 6476.

(12) Chollakup, R.; Beck, J. B.; Dirnberger, K.; Tirrell, M.; Eisenbach, C. D. *Macromolecules* **2013**, *46*, 2376.

(13) Wang, Y.; Kimura, K.; Huang, Q.; Dubin, P. L.; Jaeger, W. *Macromolecules* **1999**, *32*, 7128.

(14) Lee, B. P.; Dalsin, J. L.; Messersmith, P. B. *Biomacromolecules* **2002**, *3*, 1038.

(15) Danner, E. W.; Kan, Y.; Hammer, M. U.; Israelachvili, J. N.; Waite, J. H. *Biochemistry* **2012**, *51*, 6511.

(16) Das, S.; Donaldson, S. H., Jr.; Kaufman, Y.; Israelachvili, J. N. *RSC Adv.* **2013**, *3*, 20405.

(17) Liu, B.; Burdine, L.; Kodadek, T. *J. Am. Chem. Soc.* **2006**, *128*, 15228.

(18) Matos-Perez, C. R.; White, J. D.; Wilker, J. J. *J. Am. Chem. Soc.* **2012**, *134*, 9498.

(19) Harrington, M. J.; Masic, A.; Holten-Andersen, N.; Waite, J. H.; Fratzl, P. *Science* **2010**, *328*, 216.

(20) Das, S.; Miller, D. R.; Kaufman, Y.; Martinez Rodriguez, N. R.; Pallaoro, A.; Harrington, M. J.; Gylys, M.; Israelachvili, J. N.; Waite, J. H. *Biomacromolecules* **2015**, *16*, 1002.

(21) Ahn, B. K.; Lee, D. W.; Israelachvili, J. N.; Waite, J. H. *Nat. Mater.* **2014**, *13*, 867.

(22) Zhong, C.; Gurry, T.; Cheng, A. A.; Downey, J.; Deng, Z.; Stultz, C. M.; Lu, T. K. *Nat. Nanotechnol.* **2014**, *9*, 858.

DOI: 10.1021/jacs.5b03827
J. Am. Chem. Soc. 2015, 137, 9214−9217